

Fig. 3 Maximum temperature for a single cuff, $\beta = 0.5$.

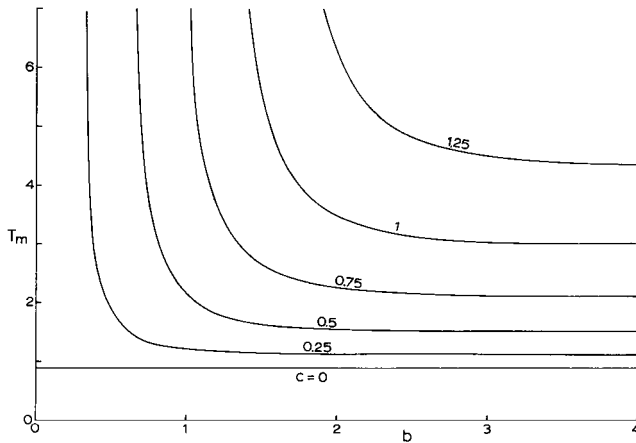


Fig. 4 Maximum temperature because of periodically placed cuffs: $\alpha = 0.5$, $\beta = 1$.

$c = 0$ curve is from Eq. (6) by setting $r = 0$. We see T_m increases dramatically as $\alpha \rightarrow \alpha_m$.

Next consider the interaction between adjacent cuffs. We shall illustrate with the case $\alpha = 0.5$, $\beta = 1$. Figure 4 shows, for large b , interaction is negligible and T_m approaches the single cuff values shown in Fig. 3. For given cuff width c , T_m becomes infinite as $b \sim c$, i.e., when the cuffs are close and prevents most of the surface heat loss. Increased cuff length c increases the interaction and thus the maximum temperature. For a given wire and a given temperature limit, the allowable length and placement of the cuff can be found. Although other values of α and β are not presented in this Note, graphs similar to Fig. 4 can be generated easily by the method outlined here.

It has been known that thermal failure (local melting) of electric heating elements in household or industrial heating is often at the hot spots because of the supports.¹ For electric overhead power lines, thermal failure is defined as an unacceptable decrease in tensile strength because of annealing. The maximum allowable temperature⁹ is set at less than 100°C. Typical values for a power line are as follows. Consider a bare copper wire of diameter 1.17 cm, carrying 200 A at 130,000 V. The resistance per centimeter is 0.000126 Ω . The power lost to Joule heating is 5.05 W/cm. Thus q_0 is 4.71 W/cm.³ Because copper $\delta = 0.004/^\circ\text{C}$ and $k = 3.86$ W/cm²/°C we find $\alpha = 0.41$. On the other hand, the Nusselt number for forced convection in crosswind is experimentally⁹ $\mathcal{O}(1)$ to $\mathcal{O}(100)$, giving a value for β from 10^{-2} to 1. The present Note provides a method to compute the maximum temperature, which may increase severalfold because of the cuffs. Last, we mention that our analysis also applies to the internal heat generated by chemical reactions.

References

- Wilcox, E. A., *Electric Heating*, McGraw-Hill, New York, 1928, Chap. 4.

- Morgan, V. T., *Thermal Behavior of Electrical Conductors*, Wiley, New York, 1991, Chap. 2.

- Carslaw, H. S., and Jaeger, J. C., *Conduction of Heat in Solids*, 2nd ed., Clarendon, Oxford, 1959, Chap. 7.

- Jakob, M., *Heat Transfer*, Vol. 1, Wiley, New York, 1940, Chap. 10.

- Jakob, M., "Temperature Distribution in Some Simple Bodies Developing or Absorbing Heat at a Linear Function of Temperature," *Transactions of American Society of Mechanical Engineers*, Vol. 70, 1948, pp. 25-30.

- Fagan, W., and Leipziger, S., "Nonuniform Cooling of a Heat-Generating Cylinder or Sphere," *Journal of Heat Transfer*, Vol. 88, Aug. 1966, pp. 257-265.

- Preckshot, G. W., and Gorman, J. W., "Steady-State Longitudinal and Radial Temperature Distribution in Internally Heated Finite Wires," *Industrial and Engineering Chemistry*, Vol. 50, No. 5, 1958, pp. 837-848.

- Douglass, D. A., "Radial and Axial Temperature Gradients in Bare Stranded Conductor," *Institute of Electrical and Electronics Engineers Transactions on Power Systems*, PWRD-1, No. 2, 1986, pp. 7-15.

- Morgan, V. T., "The Thermal Rating of Overhead-Line Conductors, Part I. The Steady-State Thermal Model," *Electric Power Systems Research*, Vol. 5, No. 2, 1982, pp. 119-139.

Characterization of Thin-Film Heat-Flux Gauges

Frank K. Lu* and Kevin M. Kinnear†

University of Texas at Arlington, Arlington, Texas 76019

Introduction

HEAT transfer can be a serious problem in applications as diverse as combustion, manufacturing, electronics, and flight. Sometimes, transient or unsteady temperature and heat transfer data are needed. These data are still obtained using discrete sensors, such as resistance temperature detectors (RTDs). An RTD consists of a thin metallic film applied to a substrate of low thermal conductivity and connected to a Wheatstone bridge.¹ The temperature change is given by

$$T - T_0 = \Delta V / \alpha_R V_0 \quad (1)$$

where ΔV is the change in the film output voltage, V_0 is the applied voltage, and α_R is the film temperature coefficient of resistance. This Note summarizes a new dynamic calibration procedure and numerical techniques for treating noisy calibration data.

RTDs are designed to satisfy the semi-infinite assumption, with a negligible effect of the thin metallic film on the substrate response. The time-varying surface temperature and heat flux are given as^{1,2}

$$T_s(t) = \frac{1}{\sqrt{\pi} \sqrt{\rho c k}} \int_0^t \frac{\dot{q}_s(\tau)}{\sqrt{t - \tau}} d\tau \quad (2)$$

$$\dot{q}_s(t) = \frac{\sqrt{\rho c k}}{\sqrt{\pi}} \int_0^t \frac{dT/d\tau}{\sqrt{t - \tau}} d\tau \quad (3)$$

where ρ , c , and k are the density, specific heat, and thermal conductivity of the film. The quantity $(\rho c k)^{1/2}$ is known as the thermal product of the film. If the heat flux is constant,

$$\dot{q}_s = \sqrt{\pi/2} \sqrt{\rho c k} / t (\Delta V / \alpha_R V_0) \quad (4)$$

Presented as Paper 98-2504 at the AIAA 20th Advanced Measurement and Ground Testing Technology Conference, Albuquerque, NM, 15-18 June 1998; received 30 September 1998; revision received 29 May 1999; accepted for publication 24 June 1999. Copyright © 1999 by Frank K. Lu and Kevin M. Kinnear. Published by the American Institute of Aeronautics and Astronautics, Inc., with permission.

*Professor and Director, Aerodynamics Research Center, Mechanical and Aerospace Engineering Department; lu@mae.uta.edu. Associate Fellow AIAA.

†Graduate Research Assistant, Aerodynamics Research Center, Mechanical and Aerospace Engineering Department; currently Senior Thermodynamics Engineer, Mechanical Systems Department, Lockheed Martin Missiles and Fire Control, Dallas, TX 75265. Member AIAA.

Equation (4) shows that the voltage change caused by the unbalanced bridge is directly proportional to the square root of time. For nonconstant heat flux, the Cook-Felderman algorithm³

$$\dot{q}_s(t_n) = \frac{\sqrt{\rho ck}}{\sqrt{\pi} \alpha_R V_0} \left\{ \frac{V(t_n)}{t_n^{0.5}} + \sum_{i=1}^{n-1} \left[\frac{V(t_n) - V(t_i)}{(t_n - t_i)^{0.5}} - \frac{V(t_n) - V(t_{i-1})}{(t_n - t_{i-1})^{0.5}} + 2 \frac{V(t_i) - V(t_{i-1})}{(t_n - t_i)^{0.5} + (t_n - t_{i-1})^{0.5}} \right] + \frac{V(t_n) - V(t_{i-1})}{\Delta t^{0.5}} \right\} \quad (5)$$

can be used to integrate Eq. (3). In Eq. (5), n is the number of equal time steps Δt .

Calibrations

Platinum RTDs on MACOR rods, 10 mm long and 1.6 mm in diameter, were constructed by hand.⁴ The temperature coefficient of resistance and the thermal product of the RTDs were obtained by calibration. Based on experiences of other investigators,¹ only RTDs with resistance between 75 and 150 Ω at room temperature were calibrated and tested.

Equation (1) indicates that the RTD sensitivity is inversely proportional to V_0 . The maximum applied voltage, however, is limited by internal heat generation. To determine this threshold, the RTD bridge was placed in still air and balanced. The current to the bridge was increased, and, eventually, the bridge became unbalanced due to ohmic heating. The output was practically nil up to an excitation of about 1 V, above which the effects of ohmic heating became apparent. However, up to an excitation of about 2 V, this heating was minimal. Larger voltages caused the internal heat generation to increase rapidly. Burnout usually occurred before an excitation of 4 V was reached. Experience indicated that a 2-V excitation is suitable in practice.

Static calibration was performed against a type-K thermocouple in a heated glycerin bath. Figure 1 shows static calibration results for a number of RTDs. The sensitivities of each of the RTDs were determined by linear least-squares fits. In each case, the correlation coefficient was better than 0.999. The good linear behavior confirms that RTDs can be used for temperature measurements. With R_0 taken at 25°C, the coefficient of resistance was obtained from

$$\alpha_R = \frac{1}{R_0} \frac{\Delta R}{\Delta T} \quad (6)$$

and its value ranged from 0.00178 to 0.00203/K $\pm 1\%$.

Dynamic calibration, utilizing a pulsed electrical excitation, was used to determine the thermal product. The RTD bridge, initially balanced, was supplied with a 6-V pulse for about 5 ms. An initial imbalance of the circuit will result in a step in the response output at the start of the test, this appearing as an infinite heat transfer rate. The bridge circuit must also be as inductance free as possible so that oscillatory responses are avoided or rapidly damped. Further,

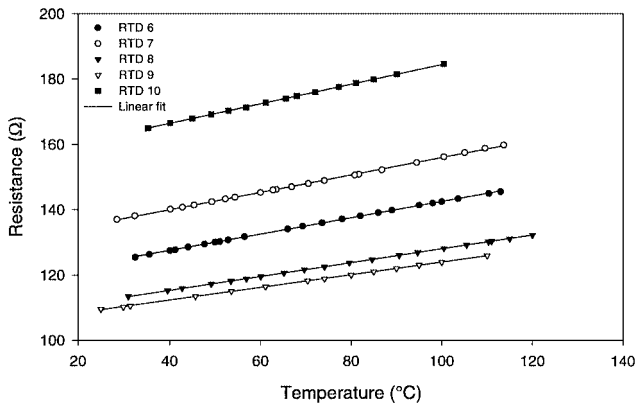


Fig. 1 Static calibration for five RTDs.

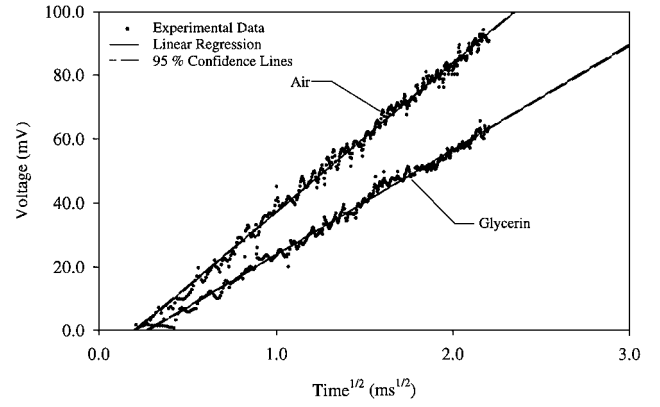


Fig. 2 Dynamic calibration results.

the 5-ms pulse was short enough to ensure the validity of the one-dimensional assumption. The pulse caused ohmic heating within the film. The change in resistance was recorded as a change in output voltage, which is equivalent to the temperature history. The test was conducted in still air and in a glycerin bath at room temperature. The parabolic behavior of the temperature rise (or output voltage) with time is indicated in Fig. 2. Figure 2 includes least-squares regressions to the data. (Approximately 500 data points were used for the least-squares analysis.) The regressions had correlation coefficients of 0.99, indicating good agreement of the measurements with theoretical parabolic behavior. The slopes of the regressions enabled the thermal product to be calculated using⁵

$$(\rho ck)^{0.5} = (\rho ck)_{\text{gly}}^{0.5} \left/ \left[\frac{(\Delta V/t^{0.5})_{\text{air}}}{(\Delta V/t^{0.5})_{\text{gly}}} - 1 \right] \right. \quad (7)$$

where the thermal product of glycerin was obtained from Ref. 1. The values of the thermal product obtained ranged from 0.190 to 0.216 J \cdot cm² \cdot K/s^{1/2}.

Testing

The RTDs were validated by measuring the stagnation-point heating in a shock tube.⁴ The tests were performed in air, initially at ambient conditions, with an incident shock Mach number of $1.79 \pm 1\%$. Figure 3a is a plot of the response of a typical RTD, including a least-squares fit, whereas Fig. 3b shows the same data after shock passage but plotted against the square root of time. The heat flux was computed from the temperature history 1) by the Cook-Felderman algorithm and 2) by assuming a constant heat flux. Figure 3a shows periodicity in the data after shock passage. This problem of ringing due to the propagation and reflection of stress waves in the RTD is a concern. In some instances, such as force measurements, elaborate data reduction procedures can be implemented to account for the propagation of stress waves. However, the high-frequency ringing cannot be effectively filtered away for the present because this procedure will increase the uncertainty in determining the starting time for heating in the RTD.

The Cook-Felderman algorithm did not converge when applied to the noisy, raw data but did succeed in calculating the heat flux from filtered data. The filtered data was in the form of a parabolic, least-squares fit for $t \geq 0$. Using this parabolic fit with the Cook-Felderman algorithm, $\dot{q}_s = 28.1$ W/cm².

Using the constant heat flux assumption, Eq. (4) was rearranged to yield

$$\Delta V = \frac{2\alpha_R V_0}{\sqrt{\pi} (\rho ck)^{1/2}} \dot{q}_s t^{1/2} \quad (8)$$

If the heat flux is constant, then the voltage change caused by the unbalanced bridge circuit is ideally proportional to the square root of time, as noted in Eq. (4) and indicated in Fig. 3b. Equation (8) can be rearranged to yield

$$\dot{q}_s = \left[(\rho ck \pi)^{1/2} / 2 \right] \lambda \quad (9)$$